THE JOURNAL OF PHYSICAL CHEMISTRY C LETTERS

2009, *113,* 17599–17603
Published on Web 09/16/2009

Conversion of Polydisperse Au Nanoparticles into Monodisperse Au_{25} Nanorods and Nanospheres

Huifeng Qian, Manzhou Zhu, Eric Lanni, Yan Zhu, Mark E. Bier, and Rongchao Jin*

Department of Chemistry, Carnegie Mellon University, Pittsburgh, Pennsylvania 15213

Received: July 30, 2009; Revised Manuscript Received: September 6, 2009

We report a facile conversion of polydisperse Au nanoparticles (1−3.5 nm) into well-defined monodisperse 25-atom (Au_{25}) nanorods and nanospheres via one-phase and two-phase thiol etching, respectively. Our method involves two main steps: first, small Au nanoparticles (polydisperse, predominantly 1−3.5 nm) were prepared by $NaBH_4$ reduction of Au(III) salt in the presence of triphenylphosphine; subsequently, these polydisperse Au nanoparticles were used as a *common* precursor for shape-controlled synthesis of Au_{25} nanorods and nanospheres following one-phase and two-phase thiol etching, respectively. Our results demonstrate that the Au_{25} particle shape can be conveniently controlled by using different types of thiol ligands in the second step of thiol etching. These ultrasmall Au_{25} nanoparticles do not support surface plasmons as do their larger counterparts (i.e., Au nanocrystals); instead, they exhibit molecular-like optical absorption behavior. This conversion process is striking in two features, size focusing and shape control, and may be extendable to the synthesis of other robust well-defined Au nanoclusters.

The recent major advances in the synthetic chemistry of nanoparticles have made it possible to prepare atomically monodisperse gold nanoparticles, at least in the ultrasmall size regime (e.g., <2 nm), using appropriate ligands such as thiols.[1−6] Unlike larger gold nanoparticles (>2 nm) that are fcc crystalline (i.e., with translational symmetry) and their optical properties are dominated by the particle plasmon excitation mode(s),[7] ultrasmall gold nanoparticles (<2 nm) do not support such surface plasmons; instead, they show molecular-like electronic structure[8] and optical properties,[8−11] intrinsic magnetism,[12,13] one-photon and two-photon fluorescence,[6,14−16] and molecular redox properties.[17−22] In the case of thiolated Au_{25} nanoparticles, a distinct HOMO−LUMO transition was observed and theoretically interpreted on the basis of the structure of $Au_{25}(SR)_{18}$.[8,23] The unique properties of gold nanoclusters are primarily caused by quantum confinement of electrons in the particle, reminiscent of semiconductor quantum dots.[24] With these new physical and chemical properties, gold nanoparticles in the ultrasmall size regime (from subnanometer to ∼2 nm) may become an important and promising type of nanomaterial for further exploration of their useful material properties for applications in catalysis, optics, electronics, and biomedicine.

Among the several reported well-defined quantum sized Au_n nanoparticles capped by thiolates (n is the number of gold atoms), the 25-atom (Au_{25}) nanoparticles are perhaps the most extensively studied system.[15,25−28] Tsukuda and co-workers reported the synthesis of mixed thiol/phosphine-protected Au_{25} nanoparticles and determined their X-ray structure to be a biicosahedral structure,[28] i.e., two icosahedral Au_{13} units joined by sharing one vertex gold atom (hence $13 \times 2 - 1 = 25$ atoms), Scheme 1A. This structure is related to the previously reported bimetal $[Au_{13}Ag_{12}(PR_3)_{10}Br_7]^{2+}$ nanocluster.[29] This type of Au_{25} nanoparticles exhibits a rodlike shape (an ultrasmall Au_{25} nanorod, 1.1 nm (length) × 0.5 nm (diameter), Scheme 1A). Very recently, we have discovered a new structure of Au_{25} nanoparticles capped by all thiolates (no phosphine ligands in the particle). X-ray crystallography unravels that the thiolated Au_{25} nanoparticle features an icosahedral Au_{13} kernel encapsulated by an exterior gold shell consisting of the remaining 12 gold atoms;[8] the entire particle exhibits a spherical shape (an ultrasmall Au_{25} nanospheres, ∼1 nm diameter), Scheme 1B. These two shapes (rod and sphere) of ultrasmall Au_{25} nanoparticles are extraordinary. With respect to their optical absorption properties, Au_{25} nanorods and nanospheres show distinct optical

SCHEME 1: Two Shapes of 25 Gold Atom (Au_{25}) Nanoparticles: (A) Biicosahedral Au_{25} Nanorods (Side and End Views); (B) Two-Shell Au_{25} Nanospheres (Redrawn from Their X-ray Crystal Structures[8,28])

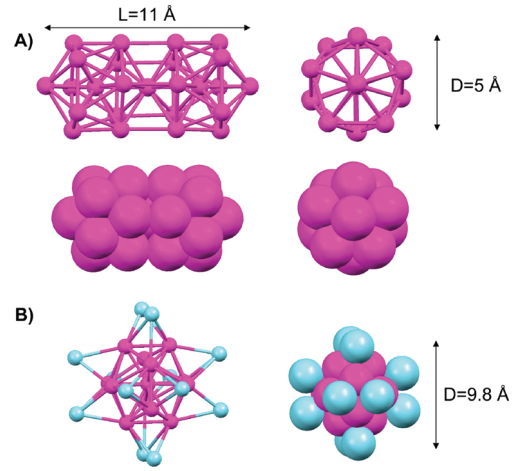

* To whom correspondence should be addressed. E-mail: rongchao@andrew.cmu.edu.

SCHEME 2: Conversion of Polydisperse Au Nanoparticles into Atomically Monodisperse Au_{25} Nanorods and Nanospheres via Respective One-Phase (a) and Two-Phase Thiol Etching (b)[a]

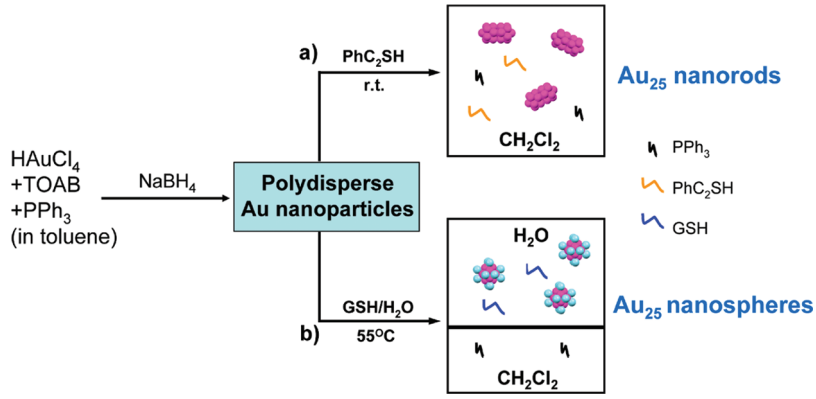

[a] CH_2Cl_2 (or $CHCl_3$) was used to dissolve the starting Au nanoparticles in both processes (a and b).

spectroscopic fingerprints that allow for convenient identification of them in synthetic work.[8,28] From the viewpoint of practical applications, it is highly desirable to develop a facile method that allows one to readily control the Au_{25} nanoparticle shape by controlling the experimental conditions.

In this work, we report a facile conversion of phosphine-capped, polydisperse Au nanoparticles (predominantly 1−3.5 nm) into rod-shaped and spherical Au_{25} nanoparticles following one-phase and two-phase thiol etching, respectively. Our method involves two main steps: first, small polydisperse Au nanoparticles were prepared in water/toluene (two phase) using $HAuCl_4$ as the metal precursor and by reduction with $NaBH_4$ in the presence of triphenylphosphine, and then, these polydisperse Au nanoparticles were isolated and used as a *common* precursor for shape-controlled synthesis of Au_{25} nanorods and nanospheres following one-phase and two-phase thiol etching, respectively, Scheme 2. Our results demonstrate that the Au_{25} nanoparticle shape can be conveniently controlled by using different types of thiol ligands in the second step of etching.

To prepare the initial Au nanoparticles, $HAuCl_4 \cdot 3H_2O$ (0.118 g, 0.3 mmol) was dissolved in 5 mL nanopure H_2O, and tetraoctylammonium bromide (TOAB, 0.190 g, 0.348 mmol) was dissolved in 10 mL of toluene. The two solutions were combined in a trineck flask. The mixture was vigorously stirred for ∼15 min to effect phase transfer of gold salt into the toluene phase through the formation of charge neutral compounds, $TOA^+[AuCl_{4-x}Br_x]^-$; the clear aqueous phase was removed. Triphenylphosphine (PPh_3, 0.235 g, 0.9 mmol) was added to the toluene solution under vigorous stirring. The solution immediately became whitish cloudy. An aqueous $NaBH_4$ solution (0.034 g, 0.9 mmol, dissolved in 5 mL of ethanol, $NaBH_4$/Au = 3:1 mol) was rapidly injected all at once into the toluene solution. The solution immediately turned dark, indicating the formation of Au nanoparticles. The reaction was allowed to proceed for 2 h at room temperature. Following rotary evaporation of toluene, a black product was obtained. The black product was washed several times with hexane to remove excess PPh_3 and TOAB, and then dissolved in CH_2Cl_2 (or $CHCl_3$) for the next step of conversion to Au_{25} nanorods and nanospheres, respectively.

The phosphine-stabilized polydisperse Au nanoparticles show a broad absorption band spanning the entire UV−vis spectrum (Figure 1A) and no prominent band at ∼520 nm was observed, indicating that the as-made phosphine-protected nanoparticles are small and consist of a mixture of different sized particles, since the absorption spectrum is quite featureless and broad.

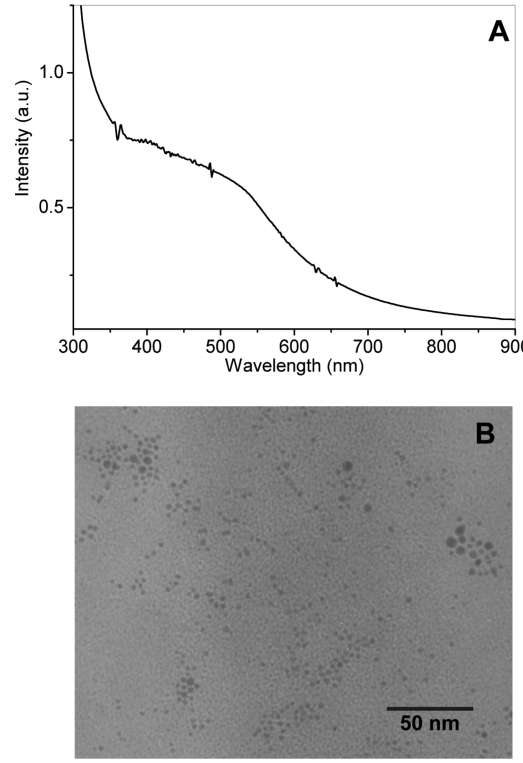

Figure 1. Phosphine-protected polydisperse Au nanoparticles synthesized in the first step: (A) UV−vis absorption spectrum; (B) TEM image.

TEM indeed showed a broad size distribution (predominantly ∼1 to ∼3.5 nm diameter) of these nanoparticles (Figure 1B). Interestingly, these polydisperse Au nanoparticles can be utilized to grow well-defined, atomically monodisperse Au_{25} nanorods and nanospheres following respective one-phase and two-phase thiol etching procedures, Scheme 2.

The conversion to Au_{25} nanorods was effected by adding PhC_2H_4SH thiol (abbreviated as PhC_2SH) to the polydisperse nanoparticles dissolved in CH_2Cl_2 (Scheme 2, route a). Briefly, 20 mg of Au nanoparticles was first dissolved in 20 mL of CH_2Cl_2; PhC_2H_4SH was then added to the solution with a molar ratio of PhC_2H_4SH/Au = 6:1. The solution was vigorously stirred at room temperature for ∼12 h. Over the time, we observed that the solution color changed from dark red to dark green, indicating a conversion of the starting nanoparticles after interacting with PhC_2H_4SH thiol in the one-phase (CH_2Cl_2)

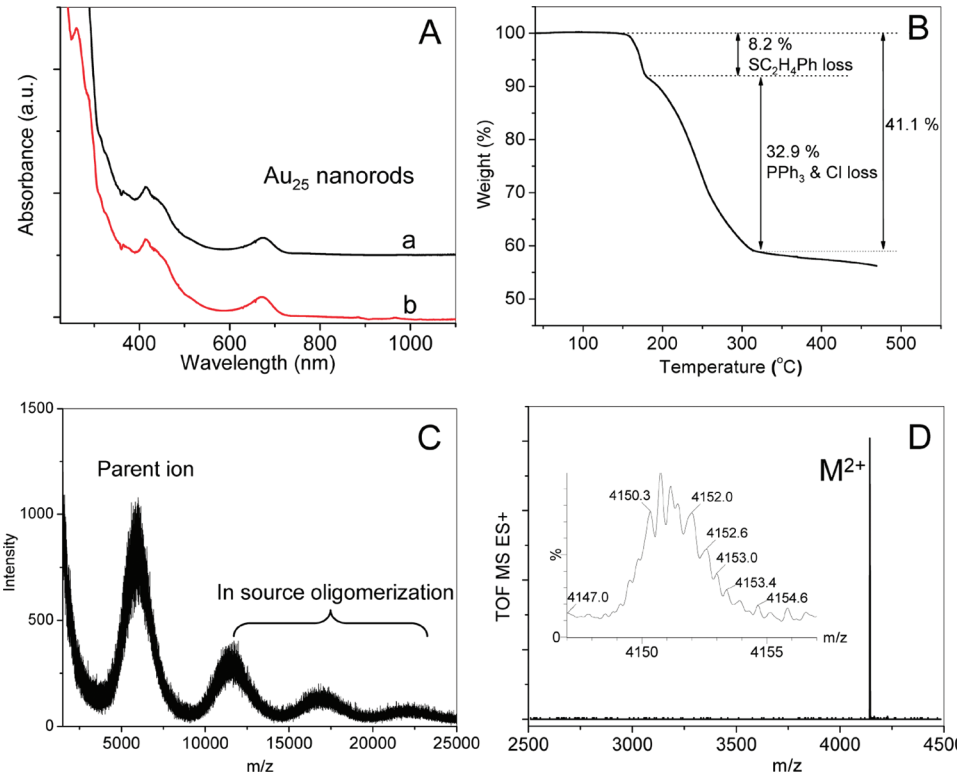

Figure 2. Conversion of polydisperse Au nanoparticles into monodisperse Au_{25} nanorods via one-phase thiol etching. (A) UV−vis absorption spectrum of the product (curve a); for comparison, the standard spectrum of Au_{25} nanorods (biicosahedron) is also shown in curve b. (B) Thermogravimetric analysis (TGA) of the product. (C) MALDI-MS spectrum of the product (matrix: sinapic acid). (D) ESI-MS spectrum of the product showing a strong peak at $m/z = 4152$ corresponding to Au_{25} nanorods with a formula of $[Au_{25}(PPh_3)_{10}(SC_2H_4Ph)_5Cl_2]^{2+}$.

system. The final product was collected after rotary evaporation of solvent (CH_2Cl_2) and subsequent extraction with ethanol.

The UV−vis absorption spectrum of the product shows a prominent peak at 670 nm and several additional bands at shorter wavelengths, including a small peak at 415 nm and a broad shoulder band at ~450 nm, Figure 2A (spectrum a). These spectral features are indeed identical to the spectroscopic fingerprints of biicosahedral Au_{25} nanorods made by following the method reported by Shichibu et al.[28] For the latter method, Shichibu et al. first made monodisperse $Au_{11}(PPh_3)_7Cl_3$ nanoclusters and then converted them to biicosahedral Au_{25} nanoparticles (formula: $[Au_{25}(PPh_3)_{10}(SC_2H_5)_5Cl_2]^{2+}$).[28] The optical absorption at ~670 nm (assigned to LUMO ← HOMO) is an electronic transition due to the dimeric structure, while the absorption peaks in the shorter wavelength region (<600 nm) are assigned to the electronic transitions within the individual Au_{13} unit.[30] The comparison of the optical spectrum of the product with the standard spectrum of $[Au_{25}(PPh_3)_{10}(SCH_2CH_3)_5Cl_2]^{2+}$ allows for an easy identification of the nanoparticles converted via the one-phase process; note that TEM imaging is not capable of resolving the rod shape of these ultrasmall nanoparticles (~1 nm). On the basis of spectral comparison, we identified that the product from the one-phase thiol etching process is biicosahedral Au_{25} nanorods and the nanoparticle composition is formulated as $[Au_{25}(PPh_3)_{10}(SC_2H_4Ph)_5Cl_2]^{2+}$ (counterion: Cl^-) in accordance with the standard $[Au_{25}(PPh_3)_{10}(SC_2H_5)_5Cl_2]^{2+}$ nanoparticle.[28] To confirm our assignment and verify the monodispersity of the as-prepared Au_{25} nanorods, we have performed thermogravimetric analysis (TGA), matrix-assisted laser desorption ionization (MALDI), and electrospray ionization (ESI) mass spectrometry analysis of the nanoparticles, Figure 2B−D.

In TGA analysis, two stages of weight loss were observed at ~170 and ~245 °C, respectively. The first loss corresponds to the five phenylethylthiolates (expected wt %, 8.2%; observed, 8.2%), while the second corresponds to the loss of 10 PPh_3 as well as Cl^- (expected wt %, 33.2%; observed, 32.9%); hence, the TGA results are consistent with the assigned $[Au_{25}(PPh_3)_{10}(SC_2H_4Ph)_5Cl_2]^{2+}$ formula. ^{1}H-NMR analysis also confirmed the PPh_3/SC_2H_4Ph ligand ratio (2:1, see Figure S1 in the Supporting Information). MALDI-MS analysis showed a mass peak centered at ~5.9 kDa (Figure 2C); apparently, ligand loss and fragmentation/recombination processes have occurred in the gas phase, which complicates the mass spectral analysis. However, intact nanoparticle signals were observed in ESI-MS analysis. A strong signal (divalent cation, evident by the ~0.5 spacing in the isotopic pattern, see Figure 2D inset) was observed at average mass $m/z = 4150.8$ (gross calibrated), which is in good agreement with the theoretical m/z value (4150 monoisotopic, 4152 average) corresponding to the assigned $[Au_{25}(PPh_3)_{10}(SC_2H_4Ph)_5Cl_2]^{2+}$ formula. Overall, the close resemblance of the optical spectrum of our product to that of the standard biicosahedral Au_{25} nanoparticles, along with the TGA results and the accurate mass measured by ESI-MS, confirms that the nanoparticles prepared in the one-phase thiol etching process are biicosahedral Au_{25} nanorods.

Interestingly, the same type of phosphine-capped polydisperse Au nanoparticles can also be utilized to make two-shell, spherical Au_{25} nanoparticles (Scheme 1B) following a *two-phase* thiol etching process (Scheme 2, route b). Briefly, an aqueous solution of glutathione (denoted as GSH, 70 mg, dissolved in 5 mL of nanopure water) was added to a CH_2Cl_2 (or $CHCl_3$) solution containing 20 mg of phosphine-capped Au nanoparticles. The reaction was conducted at ~55 °C in order to enhance the phase transfer efficiency. After the reaction was done, the aqueous phase was separated and dried by rotary evaporation. The as-obtained product was washed with methanol and then redissolved in water for UV−vis spectral measurement.

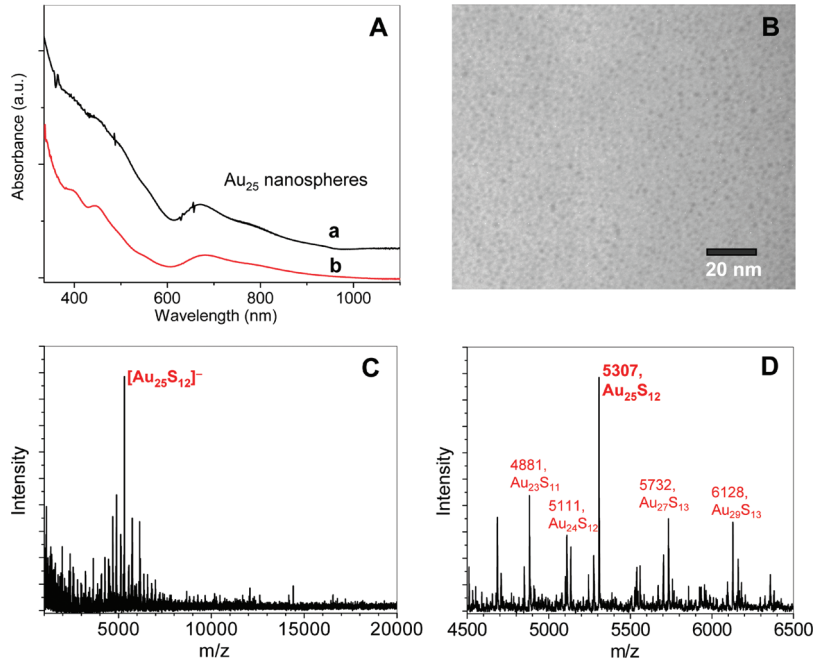

Figure 3. Conversion of polydisperse Au nanoparticles into Au_{25} nanospheres via two-phase (water/CH_2Cl_2 or $CHCl_3$) thiol etching. (A) UV−vis spectrum of Au_{25} nanospheres (curve a); for comparison, the standard spectrum of $Au_{25}(SR)_{18}$ nanospheres (two-shell structure) is also shown in curve b. (B) TEM of Au_{25} nanospheres (∼1 nm) prepared in this work. (C) MALDI-MS spectrum of $Au_{25}(SG)_{18}$ (negative ion mode, matrix: 2,5-dihydroxybenzoic acid, DHB). (D) Zoomed-in mass spectrum of $Au_{25}(SG)_{18}$.

Since different-shaped Au_{25} nanoparticles exhibit characteristic spectroscopic features,[8,28] one can readily identify them by comparing their optical spectra with standard spectra. The UV−vis spectrum of the two-phase thiol etched product was shown in Figure 3A (curve a). The product shows a distinct band centered at ∼680 nm (assigned to the HOMO−LUMO transition),[8,23,34,35] a broad shoulder band at ∼800 nm, and additional bands at 450 and 400 nm. The HOMO−LUMO transition (680 nm band) occurs in the Au_{13} core of the Au_{25} nanosphere, which is essentially an intraband (*sp* ← sp) transition, while the 450 nm band consists of mixed intraband (sp ← sp) and interband (sp ← d) transitions, and the 400 nm band arises principally from an interband transition.[8,23] Of note, the 680 nm peak in the absorption spectrum of Au_{25} nanospheres can be viewed as a transition that is due entirely to the electronic and geometric structure of the Au_{13} core.[8,23] This is strikingly different from the Au_{25} biicosahedral structure; the latter shows a similar low energy band at 670 nm, but its origin is attributed to the interaction between the two vertex-sharing Au_{13} icosahedra rather than the electronic transition within the individual Au_{13} unit.[30] These results clearly demonstrate that the particle shape of Au_{25} nanoparticles determines their optical properties. Overall, the fine spectral features of the product match well the spectroscopic fingerprints of thiolate-protected $Au_{25}(SC_2H_4Ph)_{18}$ or $Au_{25}(SG)_{18}$ nanospheres[8,15,31] (comparing spectrum a and standard spectrum b in Figure 3A). The two superimposable spectra strongly support that the nanoparticles made from the two-phase thiol etching process are spherical Au_{25} nanoparticles. TEM imaging shows the product is monodisperse and the nanoparticle size is ∼1 nm (Figure 3B). Mass spectrometry analysis also confirms the $Au_{25}(SG)_{18}$ assignment. A distict signal was observed at *m*/*z* 5307 (assigned $Au_{25}S_{12}$), Figure 3C,D. The loss of six −SG presumably corresponds to the exterior thiolate ligands (six in total), but the mechanism is not yet well understood; nevertheless, the MALDI result is almost identical to that of standard $Au_{25}(SG)_{18}$ or $Au_{25}(SC_2H_4Ph)_{18}$ particles,[4b,31] thus, confirming the particles in the product are thiolate-protected, two-shell $Au_{25}(SR)_{18}$ nanospheres.

Compared to the previous reports on phosphine-to-thiol ligand exchange using monodisperse Au_{11} nanoclusters as the starting material,[18,28,32,33] our work demonstrates that *polydisperse* Au nanoparticles can be used to synthesize monodisperse well-defined Au_{25} nanorods and nanospheres effected by appropriate thiol ligands.

Our process is striking in two features: size focusing and shape control. The facile conversion of polydisperse Au nanoparticles into atomically monodisperse Au_{25} nanorods and nanospheres via respective one-phase and two-phase thiol etching is remarkable. The conversion mechanism has not been fully understood; nevertheless, it is worth a brief discussion herein. We believe that the primary factor that determines the shape of Au_{25} nanoparticles is due to the ligand(s) present in the etching process. In the one-phase procedure, the added thiol (PhC_2H_4SH) attacks the Au nanoparticles capped by phosphines (PPh_3). The gold core fission seems to occur, since the starting polydisperse nanoparticles contain particles much larger than Au_{25} (∼1 nm). Since PPh_3 ligands are still present in the CH_2Cl_2 phase, they may rebind to the newly formed Au nanoparticles. The phosphine ligands tend to form terminal bonds with gold. The concurrent interactions of two types of ligands (i.e., PPh_3 and PhC_2H_4SH) seem to play an important role in the formation of biicosahedral Au_{25} nanorods. This concurrent interaction is inferred from the presence of both PPh_3 and PhC_2H_4SH ligands in the final Au_{25} nanorods that are formulated as $[Au_{25}(PPh_3)_{10}(SC_2H_4Ph)_5Cl_2]^{2+}$. It remains to be understood as to why the concurrent interaction of PPh_3 and PhC_2H_4SH with gold particles and their specific bonding requirements (terminal mode of phosphine verus bridging mode of thiolate) result in biicosahedral Au_{25} nanorods.

For the two-phase etching process, the reaction apparently occurs at the CH_2Cl_2/water interface, since GSH is only soluble in water and cannot enter the organic phase. The PPh_3 molecules that are detached off the starting Au nanoparticles must remain in the CH_2Cl_2 phase; therefore, the final nanoparticles in the water phase only contain hydrophilic GS− thiolates. The *sole* thiol environment results in favorable growth of the two-shell

spherical Au_{25} nanoparticles. As to the mechanism for why 25-atom gold nanoparticles instead of other sizes resulted, it may be related to the extraordinary stability of these Au_{25} nanoparticles; i.e., the conversion process might be driven in part by the particular stability of Au_{25} nanoparticles (both Au_{25} rods and spheres). More detailed information is to be learned in future study on the conversion mechanism.

In summary, we have developed a facile method for converting phosphine-capped, polydisperse Au nanoparticles (1−3.5 nm, as a *common* precursor) into ultrasmall Au_{25} nanorods (∼1 nm × 0.5 nm) and nanospheres (∼1 nm) following thiol etching in one phase and two phases, respectively. The Au_{25} nanorods are produced by the one-phase (CH_2Cl_2) thiol etching process and are stabilized by mixed phosphine and thiolate ligands (such as PhC_2H_4-SH), while the spherical (two-shell) Au_{25} nanoparticles are obtained via a two-phase (H_2O/CH_2Cl_2 or $CHCl_3$) process involving hydrophilic GSH thiol. This conversion process is unusual, as it converts polydisperse nanoparticles into well-defined, atomically monodisperse nanoparticles with precise control over particle shape. This method may be extendable to the synthesis of other ultrasmall Au_n nanoparticles, hence making this approach of potential broad utility and also expending the potpourri of useful nanoscale building blocks for future applications.

Acknowledgment. This work is financially supported by CMU, AFOSR, and PITA. We thank Dr. Joseph Suhan for assistance with TEM imaging.

Supporting Information Available: Detailed information about the synthesis and characterization of Au nanoparticles and Figure S1 showing the NMR of Au_{25} nanorods. This material is available free of charge via the Internet at http://pubs.acs.org.

References and Notes

(1) (a) Schaaff, T. G.; Shafigullin, M. N.; Khoury, J. T.; Vezmar, I.; Whetten, R. L.; Cullen, W. G.; First, P. N.; Gutierrez-Wing, C.; Ascensio, J.; JoseYacaman, M. J. *J. Phys. Chem. B* **1997**, *101*, 7885. (b) Price, R. C.; Whetten, R. L. *J. Phys. Chem. B* **2006**, *110*, 22166. (c) Hussain, I.; Graham, S.; Wang, Z.; Tan, B.; Sherrington, D. C.; Rannard, S. P.; Cooper, A. I.; Brust, M. *J. Am. Chem. Soc.* **2005**, *127*, 16398. (d) Mednikov, E. G.; Dahl, L. F. *J. Am. Chem. Soc.* **2008**, *130*, 14813. (e) Mondloch, J. E.; Yan, X.; Finke, R. G. *J. Am. Chem. Soc.* **2009**, *131*, 6389.

(2) (a) Fields-Zinna, C. A.; Crowe, M. C.; Dass, A.; Weaver, J. E. F.; Murray, R. W. *Langmuir* **2009**, *25*, 7704. (b) Kim, J.; Lema, K.; Ukaigwe, M.; Lee, D. *Langmuir* **2007**, *23*, 7853. (c) Lo, C. K.; Paau, M. C.; Xiao, D.; Choi, M. M. F. *Anal. Chem.* **2008**, *80*, 2439. (d) Dass, A. *J. Am. Chem. Soc.* **2009**, *131*, 11666.

(3) (a) Negishi, Y.; Chaki, N. K.; Shichibu, Y.; Whetten, R. L.; Tsukuda, T. *J. Am. Chem. Soc.* **2007**, *129*, 11322. (b) Muhammed, M. A. H.; Shaw, A. K.; Pal, S. K.; Pradeep, T. *J. Phys. Chem. C* **2008**, *112*, 14324. (c) Nishida, N.; Yao, H.; Ueda, T.; Sasaki, A.; Kimura, K. *Chem. Mater.* **2007**, *19*, 2831. (d) Gies, A. P.; Hercules, D. M.; Gerdon, A. E.; Cliffel, D. E. *J. Am. Chem. Soc.* **2007**, *129*, 1095. (e) Kimura, K.; Sugimoto, N.; Sato, S.; Yao, H.; Negishi, Y.; Tsukuda, T. *J. Phys. Chem. C* **2009**, *113*, 10476. (f) Yao, H.; Fukui, T.; Kimura, K. *J. Phys. Chem. C* **2008**, *112*, 16281. (g) Gautier, C.; Bürgi, T. *J. Am. Chem. Soc.* **2006**, *128*, 11079.

(4) (a) Zhu, M.; Qian, H.; Jin, R. *J. Am. Chem. Soc.* **2009**, *131*, 7220. (b) Wu, Z.; Suhan, J.; Jin, R. *J. Mater. Chem.* **2009**, *19*, 622. (c) Qian, H.; Zhu, M.; Andersen, U. N.; Jin, R. *J. Phys. Chem. A* **2009**, *113*, 4281.

(5) (a) Ackerson, C. J.; Jadzinsky, P. D.; Kornberg, R. D. *J. Am. Chem. Soc.* **2005**, *127*, 6550. (b) Jadzinsky, P. D.; Calero, G.; Ackerson, C. J.; Bushnell, D. A.; Kornberg, R. D. *Science* **2007**, *318*, 430. (c) Gao, Y.; Shao, N.; Zeng, X. C. *ACS Nano* **2008**, *2*, 1497.

(6) (a) Zheng, J.; Petty, J. T.; Dickson, R. M. *J. Am. Chem. Soc.* **2003**, *125*, 7780. (b) Bao, Y.; Zhong, C.; Vu, D. M.; Temirov, J. P.; Dyer, R. B.; Martinez, J. S. *J. Phys. Chem. C* **2007**, *111*, 12194. (c) Sakamoto, M.; Tachikawa, T.; Fujitsuka, M.; Majima, T. *J. Am. Chem. Soc.* **2009**, *131*, 6. (d) Lin, C.-A. J.; Yang, T.-Y.; Lee, C.-H.; Huang, S. H.; Sperling, R. A.; Zanella, M.; Li, J. K.; Shen, J.-L.; Wang, H.-H.; Yeh, H.-I.; Parak, W. J.; Chang, W. H. *ACS Nano* **2009**, *3*, 395–401. (e) Liu, X.; Li, C.; Xu, J.; Lv, J.; Zhu, M.; Guo, Y.; Cui, S.; Liu, H.; Wang, S.; Li, Y. *J. Phys. Chem. C* **2008**, *112*, 10778. (f) Xie, J.; Zheng, Y.; Ying, J. Y. *J. Am. Chem. Soc.* **2009**, *131*, 888.

(7) Kelly, K. L.; Coronado, E.; Zhao, L. L.; Schatz, G. C. *J. Phys. Chem. B* **2003**, *107*, 668.

(8) (a) Zhu, M. Z.; Aikens, C. M.; Hollander, F. J.; Schatz, G. C.; Jin, R. *J. Am. Chem. Soc.* **2008**, *130*, 5883. (b) Zhu, M. Z.; Eckenhoff, W. T.; Pintauer, T.; Jin, R. *J. Phys. Chem. C* **2008**, *112*, 14221.

(9) Wyrwas, R. B.; Alvarez, M. M.; Khoury, J. T.; Price, R. C.; Schaaff, T. G.; Whetten, R. L. *Eur. Phys. J. D* **2007**, *43*, 91.

(10) Negishi, Y.; Takasugi, Y.; Sato, S.; Yao, H.; Kimura, K.; Tsukuda, T. *J. Am. Chem. Soc.* **2004**, *126*, 6518.

(11) Lee, D.; Donkers, R. L.; Wang, G.; Harper, A. S.; Murray, R. W. *J. Am. Chem. Soc.* **2004**, *126*, 6193.

(12) Zhu, M.; Aikens, C. M.; Hendrich, M. P.; Gupta, R.; Qian, H.; Schatz, G. C.; Jin, R. *J. Am. Chem. Soc.* **2009**, *131*, 2490.

(13) Negishi, Y.; Tsunoyama, H.; Suzuki, M.; Kawamura, N.; Matsushita, M. M.; Maruyama, K.; Sugawara, T.; Yokoyama, T.; Tsukuda, T. *J. Am. Chem. Soc.* **2006**, *128*, 12034.

(14) (a) Link, S.; Beeby, A.; FitzGerald, S.; El-Sayed, M. A.; Schaaff, T. G.; Whetten, R. L. *J. Phys. Chem. B* **2002**, *106*, 3410. (b) Wang, G.; Huang, T.; Murray, R. W.; Menard, L.; Nuzzo, R. G. *J. Am. Chem. Soc.* **2005**, *127*, 812.

(15) Negishi, Y.; Nobusada, K.; Tsukuda, T. *J. Am. Chem. Soc.* **2005**, *127*, 5261.

(16) Ramakrishna, G.; Varnavski, O.; Kim, J.; Lee, D.; Goodson, T. *J. Am. Chem. Soc.* **2008**, *130*, 5032.

(17) Murray, R. W. *Chem. Rev.* **2008**, *108*, 2688.

(18) Yang, Y.; Chen, S. *Nano Lett.* **2003**, *3*, 75.

(19) Quinn, B. M.; Liljeroth, P.; Ruiz, V.; Laaksonen, T.; Kontturi, K. *J. Am. Chem. Soc.* **2003**, *125*, 6644.

(20) Antonello, S.; Holm, A. H.; Instuli, E.; Maran, F. *J. Am. Chem. Soc.* **2007**, *129*, 9836.

(21) Garca-Raya, D.; Madueo, R.; Blzquez, M.; Pineda, T. *J. Phys. Chem. C* **2009**, *113*, 8756.

(22) Kim, J.; Lee, D. *J. Am. Chem. Soc.* **2006**, *128*, 4518.

(23) Aikens, C. M. *J. Phys. Chem. C* **2008**, *112*, 19797.

(24) Cao, Y. C.; Wang, J. *J. Am. Chem. Soc.* **2004**, *126*, 14336.

(25) (a) Schaaff, T. G.; Whetten, R. L. *J. Phys. Chem. B* **1999**, *103*, 9394. (b) Price, R. C.; Whetten, R. L. *J. Am. Chem. Soc.* **2005**, *127*, 13750.

(26) Heaven, M. W.; Dass, A.; White, P. S.; Holt, K. M.; Murray, R. W. *J. Am. Chem. Soc.* **2008**, *130*, 3754.

(27) Zhu, M. Z.; Lanni, E.; Garg, N.; Bier, M. E.; Jin, R. *J. Am. Chem. Soc.* **2008**, *130*, 1138.

(28) Shichibu, Y.; Negishi, Y.; Watanabe, T.; Chaki, N. K.; Kawaguchi, H.; Tsukuda, T. *J. Phys. Chem. C* **2007**, *111*, 7845.

(29) Teo, B. K.; Shi, X.; Zhang, H. *J. Am. Chem. Soc.* **1991**, *113*, 4329.

(30) Nobusada, K.; Iwasa, T. *J. Phys. Chem. C* **2007**, *111*, 14279.

(31) Wu, Z.; Gayathri, C.; Gil, R.; Jin, R. *J. Am. Chem. Soc.* **2009**, *131*, 6535.

(32) (a) Woehrle, G. H.; Warner, M. G.; Hutchison, J. E. *J. Phys. Chem. B* **2002**, *106*, 9979. (b) Woehrle, G. H.; Hutchison, J. E. *Inorg. Chem.* **2005**, *44*, 6149.

(33) Shichibu, Y.; Negishi, Y.; Tsukuda, T.; Teranishi, T. *J. Am. Chem. Soc.* **2005**, *127*, 13464.

(34) Akola, J.; Walter, M.; Whetten, R. L.; Hakkinen, H.; Gronbeck, H. *J. Am. Chem. Soc.* **2008**, *130*, 3756.

(35) Jiang, D.-e.; Dai, S. *Inorg. Chem.* **2009**, *48*, 2720.

JP9073152